

NUMERICAL STUDY OF CONJUGATE NATURAL CONVECTION OVER VERTICAL FLAT PLATE WITH PROTRUDING HEAT SOURCES

Henrique L. Castro

André D. Rocha

henrique.castro@ufabc.edu.br

a.damiani@ufabc.edu.br

Energy Engineering Modeling and Simulation Laboratory (EEMSL)

Center for Engineering, Modeling and Applied Social Sciences

Federal University of ABC

Av. Dos Estados 5001, 09210-580, Santo André/SP, Brazil

Marcelo M. Ganzarolli

ganza@fem.unicamp.br

School of Mechanical Engineering

University of Campinas

Abstract. The paper presents a numerical simulation of conjugate natural-convection heat transfer from protruding heat sources in a flat plate mounted vertically. This problem arises as a typical concern of designing electronic systems that involves buoyancy-driven flows above heat sources modules. The main objective is to apply a methodology to validate numerical results for vertical position using a bi-dimensional, steady state, finite-volume method and to obtain dynamic and thermal fields. The plate contains seven elements uniformly distributed at the upper surface and an insulation layer at the bottom guaranteeing convection mechanism in only one side of the sources. Fluid physical properties are assumed uniform except for the buoyancy terms, which are obtained from the Boussinesq approximation of Navier-Stokes equations. Heat conduction in the plate is accounted in addition to convection and radiation in order to evaluate heat transfer mechanisms and non-dimensional parameters. Three different power inputs were simulated and evaluated using temperature distributions and Nu distribution around the sources

Keywords: conjugate natural convection, protruding elements, numerical simulation

1 Introduction

In numerous applications of cooling electronic components, telecom products and solar energy systems is usual the presence of clusters or single plates with heat-dissipating elements. As a natural consequence of heat dissipation to the neighboring fluid, buoyance force appears in presence of a gravitational field modifying fluid dynamic and thermal fields around these sources. Temperature control plays a major role in electronics cooling context, since the trend of miniaturization and higher power components are leading systems towards more efficient designs. Using only natural convection as a method of cooling is strategic, since it does not require an external power source to promote convection it makes the system more reliable and in some cases cheaper. Aiming to understand heat transfer mechanisms in these contexts implies not only in natural convection, but often in conduction and radiation as well. The study of convection and conduction together is known as conjugate convection and it has an important role in the analysis. Radiation effects are also significant, since the magnitudes of heat transfer coefficients encountered in many natural convection problems are in similar scale.

Natural convection around one protruding source were largely investigated, highlighted at [1-3]. Kang and Jaluria [1] performed an experimental study of natural convection flow in presence of one heated element mounted in a vertical and horizontal plate. They claimed that plate position establishes a direct effect in heat transfer downstream to the plate due to plume risen. Additionally, was discovered a strong dependence on module aspect ratio, Grashof number and temperature rise. Desrayaud and Fichra [2] proposed a correlation for the temperature and protrusion of one heated element inside an insulated channel. They varied flow Rayleigh number, module width and height, predicting an error of 5 % in the estimation of numerical data. The correlation showed a strong dependence of module width since heat flux input is proportional to the module's surface area.

Many studies have introduced an array of sources up to three elements, experimenting and numerically analyzing different regimes such as forced, mixed, laminar and turbulent configurations in [3-6]. Burak et al. [3] studied natural convection on a vertical heated plate with one, two and three heated steps. They discovered that the separation of boundary layer over the step originates a rotating flow between the elements. Moreover, they analyzed the effect of spacing between steps, finding that the predominating mechanism in the cavities is heat conduction in the plate with larger gaps. Silva, Lorente and Bejan [4] investigated the optimal distribution of discrete heat sources in natural convection. Aiming to maximize global conductance between wall and fluid they applied a methodology for sources mounted in plate and inside an enclosure. Two of the main findings are that the non-uniform spacing leads to the optimal distribution and this result depends on the Rayleigh number. Their analyses showed that sources should be positioned together if located in the boundary layer development region and if after, gaps should increase moving towards the end of the plate. Bessaih and Kadja [5], used a numerical method to simulate natural convection of three heated components in vertical channels with adiabatic walls, together with $k-\epsilon$ turbulence mode, they obtained thermal and dynamic fields. The study demonstrated that the temperature over the elements are uniform and that increasing spaces between sources enhance cooling. Another effect was discovered by using non-powered elements in an array of three elements, showing that non-powered elements benefits heat transfer in the sources next to it, downstream the domain. Boutina and Bessiah [6], performed a numerical simulation of laminar mixed convection inside a channel in presence of two heated elements modifying channel inclination, source dimension, distance between sources and inlet velocity. As expected, they validate that higher Reynolds number and source separation improves cooling. Regarding the inclination, 45 degrees case showed the highest averaged Nusselt number. Additionally, they proposed an averaged Nusselt number correlation comprising the separation and height of the sources.

Similarly, other papers conducted simulations modifying channel geometries and increasing the number of protrusions to four and five, [7-10]. Bhowmik, Tso and Tou [7], organized a three-dimensional experimental and numerical study of a vertical channel with four chips in line. Laminar flow, under natural, mixed and forced convection regimes were assessed using water as working fluid and verifying the influence of heat flux and flow rates. The results showed a great impact of Reynolds number in Nusselt number. Transitioning from forced to mixed convection thermal instabilities appeared, suggested by the authors due to secondary flow development at first three chips. In addition,

an overall correlation were presented relating Nusselt number and non-dimensional parameters such as Reynolds and Grashof numbers. Premachandran and Balaji [8] investigated two-dimensional conjugate mixed convection in a vertical channel with four equal heating sources. The numerical study considered constant geometric parameters of channel and protruding elements accounting for radiation heat transfer. Modifying mixed convection parameters such as Grashof number and Reynolds number the study added the influence of channel and source walls emissivity. Moreover, different wall/ fluid conductivity ratios were studied. Regarding radiation heat transfer, it was found to be a relevant mechanism when Reynolds number are low, around 250 and for temperatures under 100 °C. In agreement with other conjugate studies, conduction showed to be indispensable to accurately predict temperature distribution. Sarper, Saglam, and Aydin [9], combined experimental and numerical to research natural convection in a vertical channel. Comparing different blockage ratios and Grashof numbers, they studied the effect on recirculating flow and other global heat transfer coefficients. Two-dimensional analysis modeled turbulence and radiation improving numerical accuracy and finding its individual contributions. The main conclusions regard recirculation intensity, blockage ratio and Grashof number. Blockage ratio affects flow regime as it increases, fluctuation increases and laminar flow tends to transition to turbulent. Flow separation intensifies average Nusselt number downstream the last protruding element. Average Nusselt number and maximum temperature should be accounted with in order to evaluate system thermal performance. Wang, Penot and Sauliner [10] published a numerical investigation on laminar conjugate convection of a vertical plate with five integrated circuits. Among the study, they discovered the impact of a higher component in the thermal and velocity distribution. In addition, other parameters such as cavity spacing and different power inputs for one element. Positioning components with different separations showed that maximum temperature is higher in the components when they are closer compared to spaced elements. Furthermore, it remains constant independent the position of the higher element. Uniform power distribution is preferred but in presence of a higher dissipating element, its best position is at inlet. Rao and Narasimham [11], presented a study in conjugate mixed convection in a series of vertical parallel plates with five powered elements attached to a substrate. Different flow conditions of Grashof and Reynolds numbers were applied in simulations obtaining temperature distributions, mass flow and local Nusselt numbers. Results revealed that heat conduction mechanism to substrate accounts for 41-47 % of the total heat generated, concluding that adiabatic boundary conditions are not appropriated even for cases of low thermal conductivity in substrates. Additionally, a correlation was developed to relate induced velocity and flow parameters.

Regarding larger arrays of heat sources, seven elements, features in [12, 13]. Avelar and Ganzarolli [12] performed an experimental and numerical study of natural convection using an array of vertical plates parallel, establishing channels with heated elements. Numerical modeling assumed a laminar, two-dimensional and at steady state condition of flow using five plates with seven elements each. Evaluating the influence of plate separations was found that higher spacing tends to lower temperature gradients. Using non-uniform heating, was noticed that the higher heated element effect other elements downstream increasing its temperature. Rocha [13], performed an experimental investigation of an array of seven equally powered and spaced protruding elements in a conductive plate. The experiment varied power and plate inclination, measuring temperature in the middle of heat sources and cavities. Using an energy heat balance in each source, other heat transfer coefficients were obtained to later establish a correlation between Nusselt and Rayleigh numbers.

The present work aims to perform a numerical investigation of seven equally powered elements with a turbulence and radiation model, portraying convection, conduction and radiation heat transfer parcels. Moreover, to describe flow patterns inside cavities and over protrusions, temperature distributions and heat transfer coefficients by using different power inputs.

Nomenclature

a	absorption coefficient
c_p	specific heat at constant pressure of air [J/kg.K]
d	separation between heat sources [m]
g	gravitational acceleration [m/s ²]
Gr_s	modified Grashof number, based on volumetric heat generation
h	convective heat transfer coefficient [W/m ² .K]
\bar{h}	averaged convective heat transfer coefficient [W/m ² .K]
k	thermal conductivity [W/m.K] and turbulent kinetic energy
l	source length [m]
L	plate length [m]
l_x, l_y	domain length in x and y direction [m]
Nu	Nusselt number
\bar{Nu}	averaged Nusselt number
p	pressure [Pa]
Pr	Prandtl number
q''	heat flux [W/m ²]
\dot{q}	heat generation [W/m ³]
Q	power [W]
Ra	Rayleigh number
S_ϕ	Source term [W/m]
T	temperature [K]
t	plate thickness [m]
u_i	velocity component [m/s]
w	plate width [m]
x, y	cartesian coordinates [m]
x_i	coordinate direction

Greek letters

β	thermal expansion coefficient of the fluid, 1/K
ε	surface emissivity
μ	dynamic viscosity [kg/m.s]
ρ	density [kg/m ³]
σ	Stefan-Boltzmann constant, 5.6697×10^{-8} W/m ² .K ⁴
σ_s	scattering coefficient
μ	dynamic viscosity [m ² /s]
δ_{ij}	Kronecker's delta

Subscripts

cond	conductive
conv	convective
tot	total
l	length direction
max	maximum
p	protruding heat source
rad	radiative
w	wall
∞	ambient reference

2 Physical Problem and mathematical model

2.1 Physical problem

The setup consists in seven identical heat sources with constant heat dissipation attached over a vertical plate as shown in Fig. 1. Heating elements are made of aluminum and are 12.25 mm height (h_p), 12.5 mm length (l_p) and spaced by a symmetrical distance (d) of 35 mm. As a two-dimensional analysis, plate, insulation and elements are assumed to have a virtual width (w) of 340 mm, pointing outwards the paper normal. Plate has 365 mm length (L) and is 1.6 mm thick (t), made of fiberglass. The plate is mounted adjacent to an insulation layer of Styrofoam with the same length L , but different thickness of 20 mm and having its left side in contact with fluid.

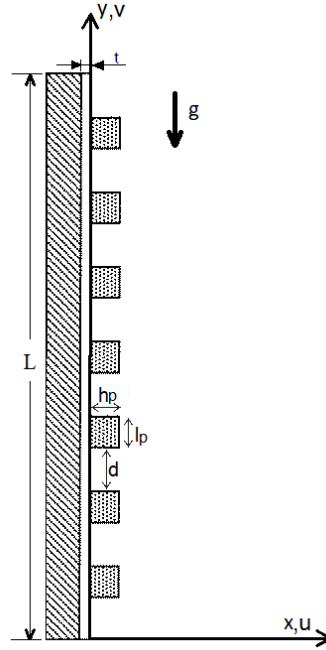


Figure 1. Schematic of the problem geometry

2.2 Governing equations

The governing equations used for simulations are based on incompressible, two-dimensional, Reynolds averaged Navier-Stokes (RANS) equations along with energy equation in dimensional form below:

continuity:

$$\frac{\partial \bar{u}_i}{\partial x_i} = 0 \quad (1)$$

momentum:

$$\rho \bar{u}_i \frac{\partial \bar{u}_i}{\partial x_j} = -\frac{\partial p}{\partial x_i} + \frac{\partial}{\partial x_j} \left[\mu \left(\frac{\partial \bar{u}_i}{\partial x_j} + \frac{\partial \bar{u}_j}{\partial x_i} \right) - \rho \overline{u'_i u'_j} \right] + \rho g_i \beta (T - T_\infty) \quad (2)$$

energy:

$$\frac{\partial}{\partial x_i} (\rho \bar{u}_i T) = \frac{\partial}{\partial x_j} \left(\frac{k}{c_p} \frac{\partial T}{\partial x_j} - \bar{u}_j \overline{T'} \right) + S_\phi \quad (3)$$

In the above equation, viscous dissipation term is neglected due to the small contribution in natural convection. Additionally, turbulence is modelled using the shear stress transport (SST) k- ω model to accurately predict near wall results as well as flow separation regions. Fluid properties are assumed constant, except for density. In momentum equation, the term $\rho \overline{u'_i u'_j}$ is denoted as Reynolds stress term and is modelled by using Boussinesq hypothesis that relate it to the mean velocity gradients, as follows:

$$\rho \overline{u'_i u'_j} = \mu_t \left(\frac{\partial \bar{u}_i}{\partial x_j} + \frac{\partial \bar{u}_j}{\partial x_i} \right) - \frac{2}{3} \rho k \delta_{ij} \quad (4)$$

Turbulent viscosity is given as:

$$\mu_t = \frac{\rho k}{\omega} \frac{a_1}{\max(a_1, \omega, SF_2)} \quad (5)$$

Turbulent kinetic energy equation:

$$\frac{\partial(\rho \bar{u}_j k)}{\partial x_j} = \bar{G}_k - \beta^* \rho \omega k + \frac{\partial}{\partial x_j} \left[\left(\mu + \frac{\mu_t}{\sigma_k} \right) \frac{\partial k}{\partial x_j} \right] \quad (6)$$

Specific dissipation rate equation:

$$\frac{\partial(\rho \bar{u}_j \omega)}{\partial x_j} = -\beta^* \rho \omega^2 + \frac{\partial}{\partial x_j} \left[\left(\mu + \frac{\mu_t}{\sigma_\omega} \right) \frac{\partial \omega}{\partial x_j} \right] + 2(1 - F1) \frac{\rho \sigma_{\omega,2}}{\omega} \frac{\partial k}{\partial x_j} \frac{\partial \omega}{\partial x_j} \quad (7)$$

SST k- ω model constants are:

$$\sigma_{k,1} = 1.176, \sigma_{\omega,1} = 2.0, \sigma_{k,2} = 1.0, \sigma_{\omega,2} = 1.168, \alpha_1 = 0.31, \beta_{i,1} = 0.075, \beta_{i,2} = 0.0828, \kappa = 0.41$$

In eq.3, the term S_ϕ represents the source term, which for the protruding elements is written as follows:

$$S_\phi = \frac{Q}{n_p \cdot w} \quad (8)$$

where Q, represents the power input, n_p is the number of elements and w width.

All thermo physical properties are evaluated at the film temperature T_f , which is defined as the average temperature of fluid maximum temperature, T_{\max} and the fluid temperature at the infinity T_∞ .

$$T_f = \frac{T_{\max} + T_\infty}{2} \quad (9)$$

Radiation transfer equation (RTE) is defined in eq.10 below by using the radiation model known as discrete ordinate (DO). This methodology solves the intensity field in the domain by integrating the RTE for a set of n different directions, defined as a numerical quadrature.

$$\frac{dI(\vec{r}, \vec{s})}{ds} = an^2 \frac{\sigma T^4}{\pi} - (a + \sigma_s) I(\vec{r}, \vec{s}) \quad (10)$$

$I(\vec{r}, \vec{s})$ is the radiation intensity, which is function of position vector \vec{r} and direction \vec{s} , a is the absorption coefficient and σ_s the scattering coefficient. The sum of the two coefficients, a and σ_s , is known as optical thickness of the medium, which for this study the fluid air is considered transparent with a and σ_s equal to zero.

2.3 Computational domain and boundary conditions

The computational domain is defined as a two dimensional volume where the width of the plate and heating sources are assumed infinitely long in paper direction. Using a commercial finite-volume based CFD solver ANSYS Fluent[®], governing equations are solved for a steady state condition and following boundary conditions. Protruding elements are defined as constant heat flux sources by introducing the source term in heat conduction equation. Heating elements and plate have all sides established as mixed convection boundary condition, which accounts for conduction and convection mechanisms. The backside of the insulation is defined as an adiabatic boundary condition. For all cases, the far-field fluid temperature is $T_{\infty}=297.29$ K.

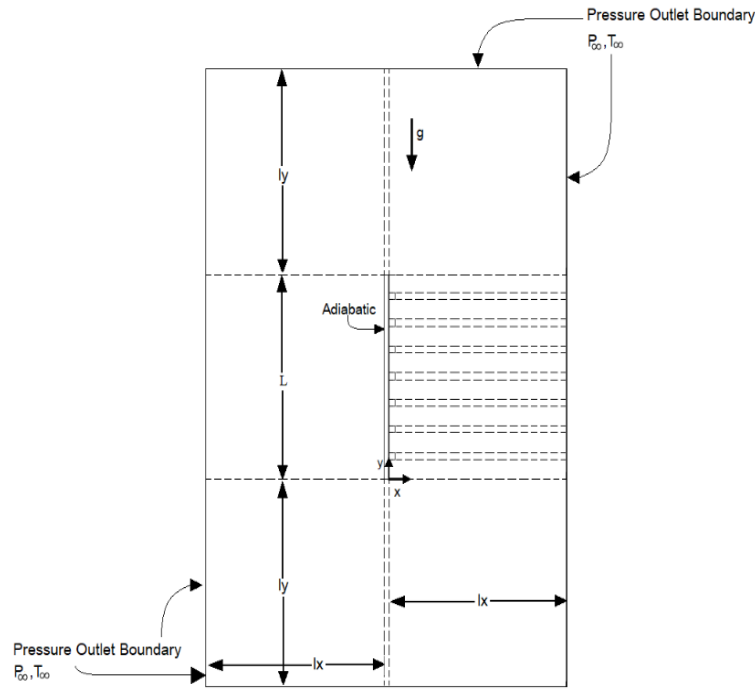


Figure 2. Computational domain and boundary conditions

All solid-fluid interfaces have no-slip boundary conditions applied. In the far-field regions, external boundaries are set as pressure outlets, which only states static pressure, temperature and allows backflow condition with this properties set in eq.11. The distance between plate and boundary is the length lx and ly measured based in the plate length (L).

$$p = p_{\infty} \text{ and } T = T_{\infty} \quad (11)$$

At solid-fluid interfaces, local net heat flux at walls is given as follows:

$$q_{wall} = -k_w \left(\frac{\partial T}{\partial l} \right)_w \quad (12)$$

Convective heat flux can be obtained by a using an energy heat balance on the surfaces, eq.13.

$$q_{conv} = q_{wall} - q_{rad} \quad (13)$$

The convective heat transfer coefficient on the surfaces is defined as:

$$h = \frac{q_{conv}}{(T_{wall} - T_{\infty})} \quad (14)$$

Averaged values of heat transfer coefficient are calculated form h and integrated over the length L_{tot} .

$$\bar{h} = \frac{1}{L_{tot}} \int_0^{L_{tot}} h \, dl. \quad (15)$$

The local and average Nusselt number are calculated using the following expressions:

$$Nu = \frac{h l_p}{k} \quad (16)$$

$$\overline{Nu} = \frac{\bar{h} l_p}{k} \quad (17)$$

Modified Grashof number, based in on volumetric heat generation is computed according to the

$$Gr_y = \frac{g\beta\dot{q}w(L/2)^3}{k v^2} \quad (18)$$

Rayleigh number:

$$Ra = Pr \cdot Gr_y \quad (19)$$

where, Pr is the Prandtl number, defined as follows:

$$Pr = \frac{\mu c_p}{k} \quad (20)$$

Table1. Thermal conductivity and surface emissivity of the materials

Component	Material	k[W/m K]	ϵ
Heat sources	Aluminum	237	0.3
Plate	Fiberglass	0.4	0.9
Insulation	Styrofoam	0.04	-
Fluid	Air	0.02662	-

Numerical Scheme

Governing equations are solved for a steady state using the pressure-velocity coupled scheme, which solves momentum and continuity equations by semi-implicit methodology. The second order upwind scheme is applied to discretize momentum, energy and turbulence model equations, and then first order to DO radiation model. Pressure interpolation is calculated using body force weighted scheme, as recommended. For continuity equation, convergence criteria is set to 10^{-5} , momentum and radiation to 10^{-6} and energy residual to the order of 10^{-9} .

Domain independence

To guarantee that further simulation results are accurate, a domain independency test was conducted. Systematically increasing the domain, by varying l_x and l_y as functions of plate length (L), simulations used the same grid structure for all cases and results are showed in Table 2.

Table 2. Computational domain convergence (Case 70 W, $Gr_y=9.4 \times 10^5$)

Computational Domain	l_x/L	l_y/L	\bar{h}_{conv}
L	1	1	2.77508
2L	2	2	2.79301
4L	4	4	2.79867

According to the data above convective heat transfer coefficient converges, relative difference in result is around 0.2 % between domains 2L and 4L. With this in mind, domain 2L is proper for simulations and compared to 4L domain it demands less computational time regarding the number of elements.

Grid independence

To ensure grid independency among results, different non-uniform structured grids were used to define finer meshes closer to wall regions and coarser distant from them. Using the method described by Celik et al. [14], three grid sizes, with an approximate geometric ratio of 1.4, were used to simulate the 2L domain size and 70 W total power dissipation case. Fig. 3 shows the grid density applied and a detailed view of the grid close to a heat source. Analyzing the convective heat transfer coefficient in table 3, is possible to affirm that it converges to an asymptotic value of 2.7798 by Richard's extrapolation and that fine grid provides an expected error around 0.1 %. Later, for all simulations ahead fine grid was employed.

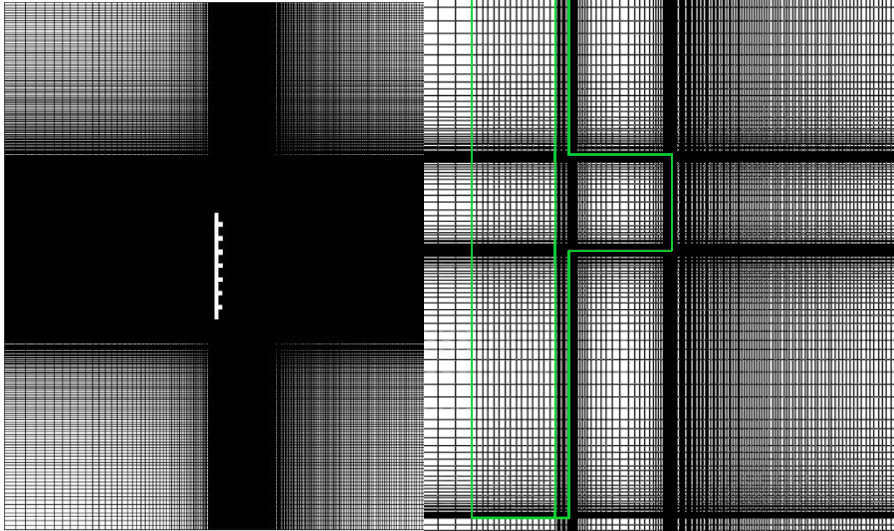


Figure 3. Grid structure and detailed view

Table 3. Grid independence test (Case 2L domain, 70 W, $Gr_y=9.4 \times 10^5$)

Grid Resolution	Grid Size	Number of Elements	\bar{h}_{conv}
Coarse	204x536	109344	2.81601
Medium	290x795	230550	2.79301
Fine	421x1196	503516	2.78438

3 Results

Conjugated natural-convection heat transfer with seven heat sources in a vertical flat plate was numerically studied. Three different power inputs (Q) were investigated, 30 W, 50 W and 70 W, which are equivalent to the following modified Grashof numbers respectively, Gr_y 4.0×10^5 , 6.7×10^5 and 9.4×10^5 . Moreover, each heat transfer mechanisms contribution were evaluated by plotting each parcel.

Temperature difference distributions along plate non-dimensional peripheral distance are shown in Fig.4 for all power input cases. Temperature is uniform at the top surface of modules and rapidly decreases towards the plate surface where it reaches the lowest values in the middle of the cavities. This result appears to be independent of heat input and position. The maximum temperature does not occurs at the last source as expected from temperature rise pattern by observing the six previous elements. As air ascends towards the plate end, it is heated and temperature difference drops between source and surrounding fluid, diminishing heat transfer. This behavior explains the crescent in temperature over the first six components and indicates that other effects are occurring in the end of the source array. Regarding power input, it seems to linear increase the gradients of temperature and temperature drop between cavities and protruding elements.

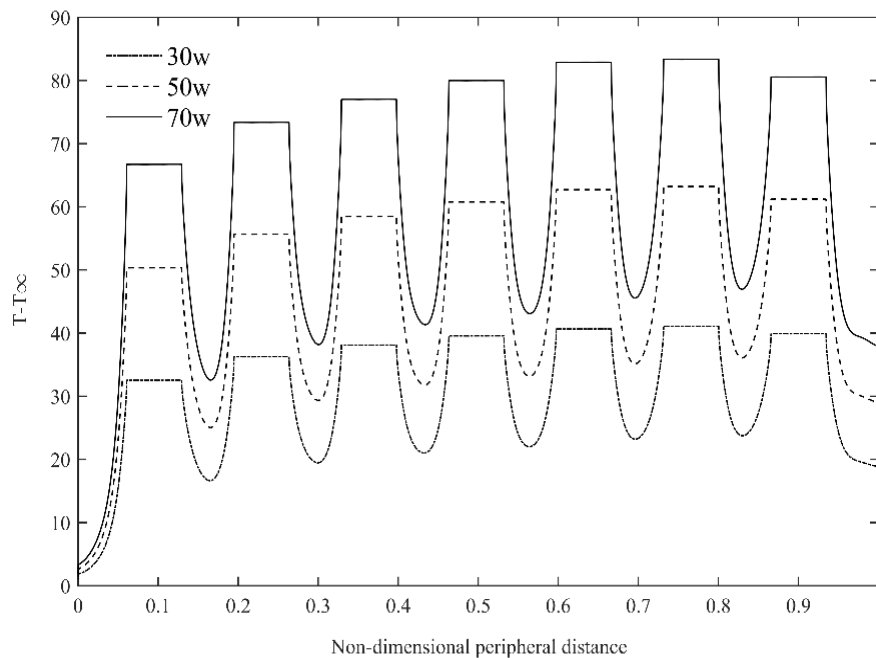


Figure 4. Temperature difference distribution

Fig.5 (a,b,c) shows the streamlines and temperature contours obtained for different source inputs. Observing the temperature of protruding components is evident that temperature is constant as consequence of the high thermal conductivity ratio between aluminum and fiberglass, approximately 600 times. First sources temperature are lower than the others because are cooled by air from inlet region at ambient temperature. Isotherms are more concentrated at the heating elements surroundings and as the Gr_y number increases thermal boundary layer decreases. At the downstream side of each source is possible to observe a slight thermal wake interacting with the opposite wall of the next element. These secondary flows or recirculation zones inside the cavities become evident when compared with the streamlines in Fig.5.

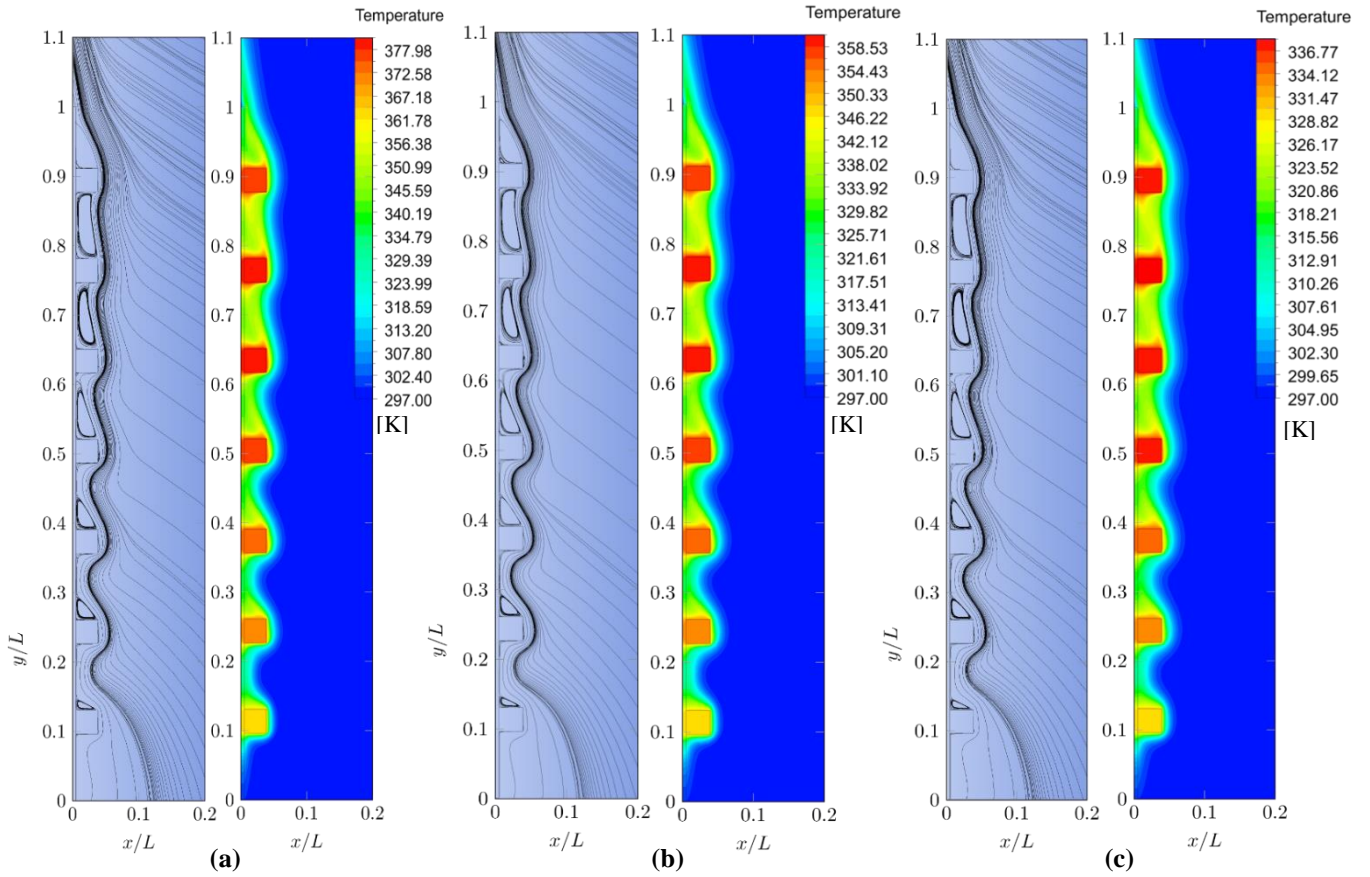


Figure 5. Streamlines and temperature contours: 70 W(a), 50 W(b), 30 W(c)

Recirculation seems to increase in eddy length towards the plate end, starting to fill the entire cavity between fifth and sixth source. Such as isotherms, streamlines are more packed as heat input grows, displaying greater gradients of velocity but only a slight intensification in recirculation zones. Regarding the smaller temperature of the last source compared to the sixth, it is proper to assume that this effect is caused by the absence of a recirculation in the last cavity of the array.

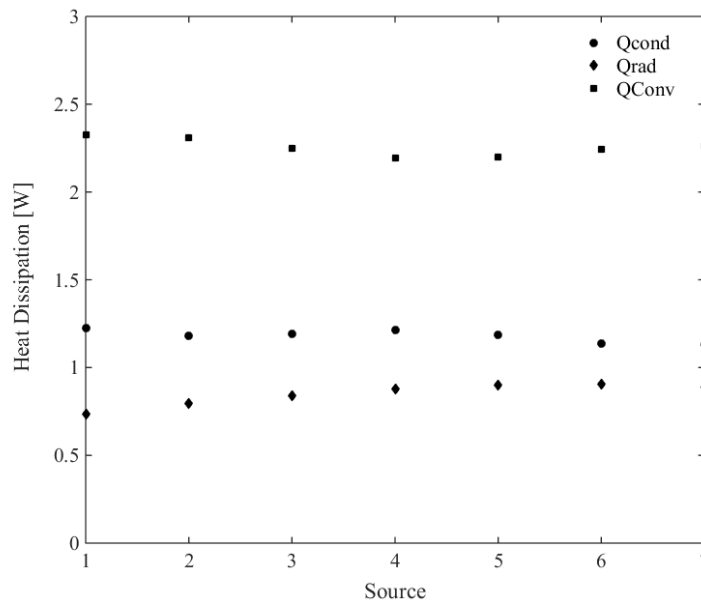


Figure 6. Power dissipation for each source element, 30 W case

A comparison of heat transfer mechanisms for each element is illustrated in Fig.6. From these results is possible to affirm that convection accounts for most of heat loss in the sources and that conduction and radiation should not be neglected in this case. Convection heat transfer occurs more intensely at the first element surroundings due to the greater temperature difference in inlet region. At the last source, despite the reduction in temperature compared to 6th source, there is a slight increase in convection. This effect might be related to the wake ascension instead of recirculating inside a cavity. Regarding radiation, heat losses gradually increases as source temperature increases. First and last elements, different from the others, receives radiation from only one adjacent source. This effect can be perceived as a drop of radiation loss in the last source, discontinuing the increasing trend that precedes it.

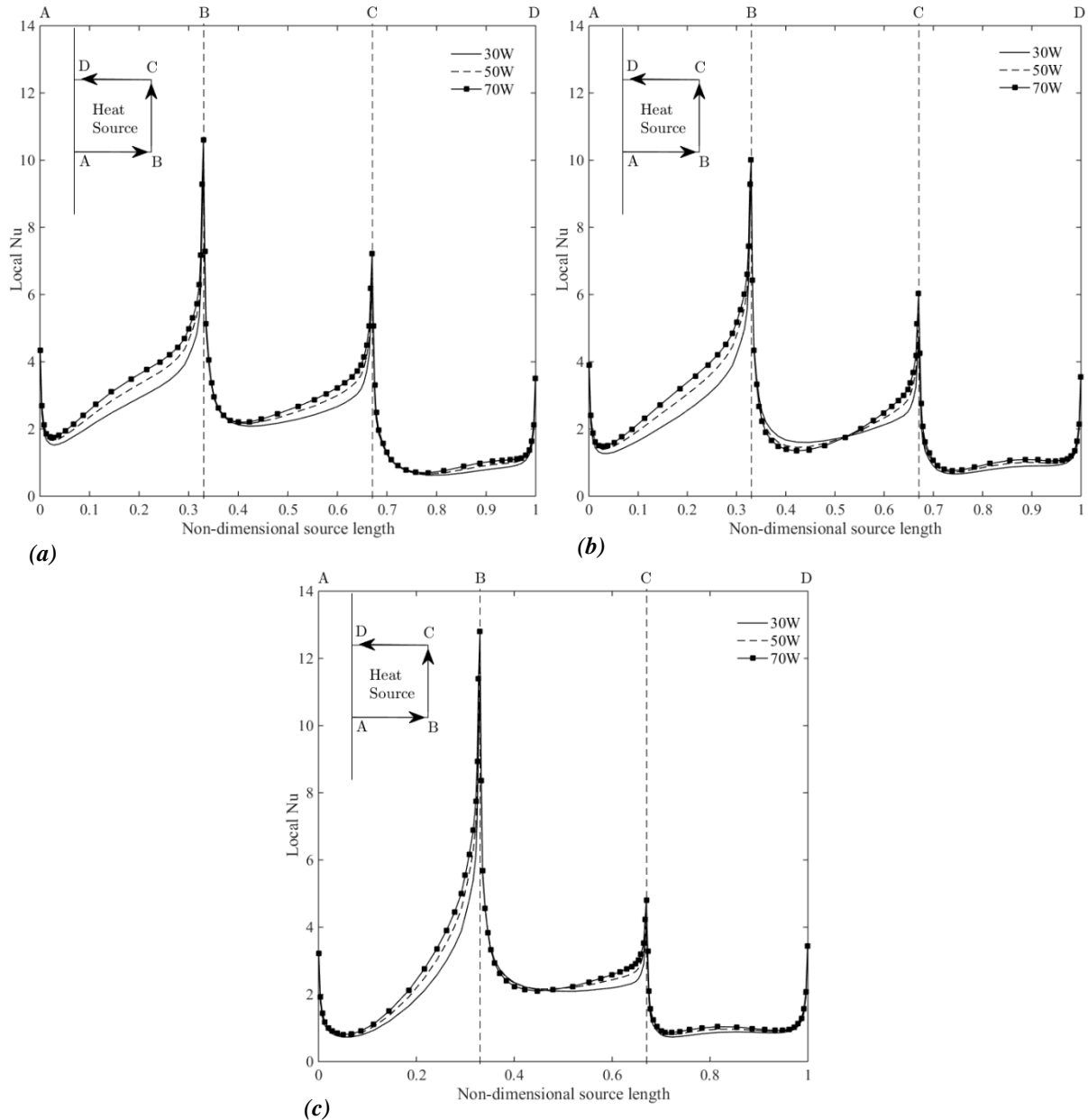


Figure 7. Local Nusselt number distributions, 2nd(a), 4th(b), 6th(c) heat sources

Fig.7 illustrates the local Nusselt number distributions for three different protruding elements, 2nd, 4th and 6th sources and three power inputs, 30 W, 50 W and 70 W. Local Nusselt distributions show peaks at the corners of modules for all position. The 2nd and 4th elements display a similar Nusselt number distribution, changing in magnitude only, it relates to the lower fluid temperatures at the entrance region. At 6th source, Nu number rapidly increases at surface AB and at BC and CD remains more stable in the central portion. Comparing the three power inputs, higher heat inputs resulted in better convective coefficient at surfaces AB and CD. At surface BC, there is a slight pattern modification in edge B among source locations and respect to power input.

4 Conclusions

The present study numerically investigates conjugated natural convection, aiming to comprehend thermo-fluid-dynamics of flow patterns adjacent to heated sources. The effect of power inputs and radiation on cooling parameters have been analyzed, giving an insight of the temperature and velocity contours behavior. Maximum temperature is found to occur at the heat source just before the last in the array and remains constant inside the element. Regarding secondary flows, streamlines and temperature contours showed recirculation induced at the cavities, which impacts in heat transfer coefficients at heat sources sides. Radiation and conduction mechanisms were examined around sources and confirmed as non neglectable for this problem. In future works, other plate inclinations are intended to be evaluated along with experimental data for validation.

Acknowledgements

This study acknowledges the Fundação de Amparo à Pesquisa do Estado de São Paulo (FAPESP), for the financial support in the project n° 2017/06978-3.

References

- [1] B.H. Kang and Y. Jaluria. Natural convection heat transfer characteristics of a protruding thermal source located on horizontal and vertical surfaces. *International Journal of Heat and Mass Transfer*, vol. 33, n.6, pp. 1347-1357, 1990.
- [2] G. Desrayaud and A. Fichera. On Natural Convective Heat Transfer in Vertical Channels With a Single Surface Mounted Heat-Flux Module. *Journal of Heat Transfer*, vol. 125, n.4, pp. 734-739, 2003.
- [3] V.S. Burak, S.V. Volkov, O.G. Martynenko, P.P. Khramtsov, I.A. Shikh. Experimental Study of Free-Convective Flow on a Vertical Plate with a Constant Heat Flux. *International Journal of Heat and Mass Transfer*, vol. 38, n.1, pp. 147-154, 1995.
- [4] A.K. da Silva, S. Lorente and A. Bejan. Optimal Distribution of Discrete Heat Sources on a Wall with Natural Convection. *International Journal of Heat and Mass Transfer*, vol.47, n.2, pp. 203-214, 2004.
- [5] R. Bessaih and M. Kadja. Turbulent Natural Convection Cooling of Electronic Components Mounted on a Vertical Channel. *Applied Thermal Engineering*, vol. 20, pp.141-154, 2000.
- [6] L. Boutina and R. Bessaih. Numerical simulation of mixed convection air-cooling of electronic components mounted in an inclined channel. *Applied Thermal Engineering*, vol. 31, n. 11–12, pp. 2052-2062, 2011.

- [7] H. Bhowmik, C.P. Tso and K.W. Tou. Analyses of Convection Heat Transfer From Discrete Heat Sources in a Vertical Rectangular Channel. *Journal of Electronic Packaging*, vol. 127, n. 3, pp. 215-222, 2005.
- [8] B. Premachandran and C. Balaji. Conjugate Mixed Convection with Surface Radiation from a Vertical Channel with Protruding Heat Sources. *Numerical Heat Transfer, Part A: Applications*, vol. 60, n. 2, pp-171-196, 2011.
- [9] B. Sarper, M. Saglam and O. Aydin. Experimental and numerical investigation of natural convection in a discretely heated vertical channel: Effect of the blockage ratio of the heat sources. *International Journal of Heat and Mass Transfer*, vol. 126, part A, pp. 894-910, 2018.
- [10] H.Y. Wang, F. Penot and J.B. Sauliner. Numerical study of a buoyancy-induced flow along a vertical plate with discretely heated integrated circuit packages. *International Journal of Heat and Mass Transfer*, vol. 40, n. 7, pp. 1509-1520, 1997.
- [11] G. M. Rao and G.S.V.L. Narasimham. Laminar conjugate mixed convection in a vertical channel with heat generating components. *International Journal of Heat and Mass Transfer*, vol. 50, n. 17-18, pp. 3561-3574, 2007.
- [12] A. C. Avelar and M. M. Ganzarolli. Natural Convection in an array of vertical channels with Two-Dimensional Heat Sources: Uniform and Non-Uniform Plate Heating. *Heat Transfer Engineering*, vol. 25, n. 7, pp. 46-56, 2004.
- [13] A. D. Rocha. Convecção Natural em Placa Nas Posições Vertical e Inclinada Contendo Elementos Protuberantes Aquecidos. Master dissertation, Faculty of Mechanical Engineering of Universidade Estadual de Campinas, 2005.
- [14] I. Celik, U. Ghia, P.J. Roache, C. Freitas, H. Coloman, P. Raad. Procedure of Estimation and Reporting of Uncertainty Due to Discretization in CFD Applications. *Journal of Fluids Engineering*, vol.130, n. 7, 2008.